Available online at www.sciencedirect.com
SCIENCE DIRECT®
International Journal of Thermal Sciences 43 (2004) 725–732
International Journal of Thermal Sciences
www.elsevier.com/locate/ijts

Computational analysis of transient heat transfer in turbulent pipe flow

Ali Cemal Benim [a,*], Markos Cagan [a], Dogan Gunes [b]

[a] *Department of Mechanical and Process Engineering, Duesseldorf University of Applied Sciences, Josef-Gockeln-Str. 9, 40474 Duesseldorf, Germany*
[b] *Department of Mechanical Engineering, Istanbul Technical University, 80191 Gümüssuyu, Istanbul, Turkey*

Received 20 August 2003; received in revised form 18 December 2003; accepted 24 February 2004

Available online 10 June 2004

Abstract

Unsteady convective heat transfer in turbulent pipe flow has been computationally investigated, by means of transient simulations, using different turbulence models. The transient analysis was preceded by a steady-state study, where no substantial differences in the performances of the considered two-equation turbulence models were observed. In the transient analysis, the main emphasis has been placed upon high Reynolds number, two-equation turbulence models, augmented by the wall-functions approach. Two-layer-zonal models, which do not utilize the wall-functions approach have also been considered for some cases. Step-like, pulse-like and sinusoidal perturbations of the flow rate at various Reynolds numbers have been analysed. Results have been compared with measurements. It has been observed that some features of the considered configurations could be predicted. On the other hand, some aspects such as the delay of the transient response of the wall heat flux to the flow rate changes could not be predicted well.

Keywords: CFD; Transient heat transfer; Turbulent pipe flow; Turbulence modelling

1. Introduction

Unsteady convective heat transfer in pipes is an important feature in a broad range of engineering devices. An improved understanding of the underlying mechanisms would further contribute to the design of such practically important devices as automotive engines and pulse combustors [1]. An enhancement of the effectiveness of heat exchangers by flow unsteadiness has also been suggested [2]. A detailed understanding of the transient convective heat transfer is important not only for the insight it provides to the mean heat transfer problem, but also in its own right, where it might find application, for example, in the design of inlet manifolds in automotive engines [3].

In analysing fluid flow problems, Computational Fluid Dynamics (CFD) based simulation procedures have gained such maturity, within the last decade, that they are now considered to be an indispensable analysis and design tool in a wide and ever-increasing range of applications. The convective heat transfer has also been analysed intensively via computational methods [4,5]. As numerical predictions of flow and heat transfer problems principally exhibit inaccuracies to some extent, quite often due to the turbulence modelling, the issue of turbulence model validation has occupied a central role in the computational analysis of flow problems. Validation of computational procedures for the convective heat transfer was already performed by several authors [6,7]. However, in such studies, the main emphasis was lying on the steady-state problems. On the other hand, validation of prediction procedures for the transient convective heat transfer has received comparably less attention. This is the scope of the present investigation.

In the present study, the convective heat transfer in unsteady turbulent pipe flow has been investigated computationally, by means of transient simulations, and the results have been validated by comparisons with the recent experiments of Barker and Williams [8].

2. Modelling

For the numerical investigations, the general purpose CFD code Fluent [9] has been used as the basis, which

* Corresponding author. Fax: + 49 (0) 211–43 51 403.
E-mail addresses: alicemal.benim@fh-duesseldorf.de (A.C. Benim), markos.cagan@fh-duesseldorf.de (M. Cagan), gunes@itu.edu.tr (D. Gunes).

1290-0729/$ – see front matter
doi:10.1016/j.ijthermalsci.2004.02.012

Nomenclature

Nu	Nusselt number
Pr	Prandtl number
q	wall heat flux
$\bar{q}$	time-averaged wall heat flux
Re	Reynolds number
t	time
T	temperature
u	axial velocity
U_c	centerline velocity
y	distance to the wall
y^+	non-dimensionalized y ($y^+ = \frac{y}{\nu}\sqrt{\frac{\tau_w}{\rho}}$)

Greek symbols

μ	dynamic viscosity
ν	kinematic viscosity
ρ	density
τ_w	wall shear stress

Subscripts

T	turbulent
L	laminar

utilizes a finite volume method to discretize the governing equations, and a pressure-correction formulation to handle the velocity-pressure coupling. Ensemble averaged (averaged over a large number of repetitions) continuity, Navier–Stokes and energy transport equations have been solved for the incompressible, unsteady, 2D, axisymmetrical, turbulent pipe flow.

2.1. Mathematical modelling

Second moment closure turbulence models [4] are not necessarily required by the rather clearly arranged fluid dynamics of the pipe flow. Since we also primarily aim to validate models, which can rather easily be used in practical applications, i.e., which do not necessarily imply a very high computational overhead, the attention has been focused, in the present study, on the validation of two-equation, turbulent viscosity models.

Different two-equation turbulence models, namely the standard k–ε model [10], the RNG k–ε model [11], and the realizable k–ε model [12] have been used. For comparison, a one-equation turbulence model [13] has also been used in the steady-state analysis. The modelling of the near-wall region is especially important in convective heat transfer problems. Several formulations including standard [10] or non-equilibrium [14] wall-functions (for bypassing this region adopting logarithmic wall-functions), and two-layer-zonal methods (adopting low Reynolds number amendments [15] to accurately resolve the near-wall region) have been considered. Although the two-layer-zonal methods principally offer a more accurate treatment of the near-wall region, their application in solving practical problems has still remained quite restricted. This is due to the fact that the very fine grid resolution of the near-wall region, required for an adequate application of such models, increases the computational overhead considerably, especially for three-dimensional problems, which would additionally be increased, in transient problems. Thus, due to their importance in practical applications, the attention has been focused on the high Reynolds number two-equation turbulence models adopting a wall-function approach, in the transient part of the present study, whereas two-layer-zonal methods have also been considered for some cases.

The solution domain of the considered 2D, axisymmetric pipe flow is geometrically quite simple, which is a rectangle on the x–r plane, enclosed by the inlet, outlet, symmetry and wall boundaries. On walls, no-slip conditions were used for the momentum equations. The wall boundary condition for the energy equation was a constant temperature, in accordance with the considered experiments.

The applied boundary condition at the inlet was the prescription of the measured velocity and temperature, whereby spatially constant profiles were assumed. The inlet velocity values have been derived from the given Reynolds numbers. Inaccuracies due to an eventual uncertainty in the shape of the inlet velocity profiles were not expected to play an important role, since all measurements were carried out at a cross-section, placed sufficiently downstream from the inlet (at a distance of approx. 40 pipe diameter), so that quite fully-developed conditions should be expected at the measuring station. For transient cases, the inlet velocity was varied in time, as prescribed by the experiments. The outlet boundary condition was the so-called "outflow" condition, which implies zero-gradient conditions at the outlet. As discussed above, given that the pipe is long enough, this should be quite convenient for the momentum equations. In the present arrangement, this has also been expected to be a reasonable condition for the energy equation. As a further modelling strategy, a total pressure specification at the inlet and a static pressure specification at the outlet were also used as boundary conditions for the momentum equations, in some computations. No measurements of the turbulence quantities were available. Thus, the inlet boundary conditions for the turbulence quantities were derived assuming a turbulence intensity of 4% and a macro mixing length of 30% pipe diameter. Although these values suffer under some uncertainty, we assume that the possible inaccuracies introduced by this choice would not substantially deteriorate the predictive capability. Since the measuring station is quite far away from the inlet, as mentioned above, an equilibrium turbulence would rather be expected there, where the inlet val-

ues of the turbulence quantities and uncertainties in their estimation should not be playing a major role.

In defining the material properties of the air, constant values were prescribed, which corresponded to an average temperature value, which was defined as the arithmetic average of the wall temperature and the estimated bulk fluid temperature at the measuring station. Since the temperature difference between the wall and the fluid was rather small, i.e., about 25–30 °C, it was considered that the neglecting of the temperature dependency of the material properties would not lead to an important loss of accuracy.

2.2. Numerical modelling

The solution domain has been prescribed to be about five pipe diameters longer than the actual pipe length, for minimising possible upstream disturbances at the measuring station due to the prescribed numerical outlet boundary condition.

The solution domain was discretized by a structured grid. The number of computational cells were tried to be adjusted in an optimal way according to the Reynolds number and the turbulence model used, and for achieving grid independent results. The computational cells used in the radial direction varied between the minimum value of 10 and maximum value of 70, in all cases considered.

In using the two-layer-zonal model, the wall-layer needs to be resolved sufficiently fine. For these computations, the near-wall cell of the grid was placed at a location where the non-dimensional wall-distance y^+ is smaller than 1.0. Then, a smooth grid expansion towards the pipe axis was applied, which, however, allowed at least 5 cells for the resolution of the viscous sub-layer, which is theoretically defined by $y^+ \leqslant 5$.

In using the wall-functions approach, it must be ensured that the near-wall cell is sufficiently far away from the wall. It is generally recommended that the condition $y^+ \geqslant 30$ should be fulfilled for the near-wall cell. However, our experience [16] indicates that the accuracy of the wall-functions start to show a remarkable deterioration beyond $y^+ <$ approx. 12. Thus, in designing the present grids, the condition of $y^+ \geqslant 30$, was preferably fulfilled. However, the condition of $y^+ \geqslant 12$, was also allowed in some extreme cases, where, otherwise a too coarse overall grid would result. Since the non-dimensional wall distance y^+ varies with the Reynolds number, the fulfilment of the above-mentioned conditions for near-wall cells resulted in different grids, for different Reynolds numbers, with different number of cells in the radial direction. Using the wall-functions, basically a uniform grid spacing was applied in the radial direction. This, however, implied a too coarse resolution in the radial direction, for low Reynolds numbers, when the wall-function requirements for the first near-wall cell are fulfilled. For such cases, the grid was refined in the core region (i.e., in the whole radial domain, except the near-wall cell), in order to have at least 10 cells in the radial direction, while keeping the first near-wall cell sufficiently away from the wall.

The number of cells used in the axial direction varied between 200 and 400. The grid was refined near the inlet, for capturing the locally high axial gradients in the entry region of the developing flow. This was followed by an equidistant spacing. Approximately 200 cells in the axial direction were found to be sufficient for grid-independent solutions. However, this number was increased for the cases with too fine radial grid resolution, for avoiding too large cell aspect ratios.

Second order schemes were used for the spatial discretization of the governing equations, for attaining a high numerical accuracy.

The equations have been integrated in time using an implicit procedure, using a constant time step for each case. However, the time step has been varied from case to case, according to the characteristics of the case considered. Similar to a grid independency study for finding out the necessary spatial resolution, transient runs with different time steps were performed for finding out the necessary temporal resolution. In several test runs, it has been found for the case of sinusoidal perturbations, that a discretization of a period by approximately 60 time steps is sufficiently accurate. Nevertheless, for the computations presented, a period was discretized even by a greater number, i.e., by 80 time steps, for ensuring sufficient accuracy for all cases. All unsteady computations have started with the steady-state solution as the initial condition. For the case of sinusoidal perturbations, attention has been paid for the development of full periodicity, before comparing the results with the experiments. Starting from a steady-state solution and perturbing it by a sinusoidal oscillation of the inlet conditions, a sufficient periodicity of the flow at the pipe exit has been observed after about 10 cycles. However, for excluding any uncertainty, at least 15 cycles have been computed for each case.

3. Results

As the experimental basis, the recent transient convective heat transfer measurements of Barker and Williams [8] have been utilized. In these experiments, the unsteady turbulent pipe flow subject to sinusoidal perturbations at different amplitudes (8–80%) and frequencies (0.5–30 Hz) was investigated. Additionally, non-sinusoidal changes of the mass flow rate were also considered. The Reynolds numbers based on the time average velocity were varying between the values 8000 and 30 000. The walls of the pipe were held at the constant temperature of approx. 80 °C by means of two heaters (one for the main length, one for the test section), which were controlled independently, using proportional integral differential controllers. Transient measurements of the velocity, temperature and the wall heat flux were performed. A sketch of the experimental set-up of Barker and Williams [8] is shown in Fig. 1.

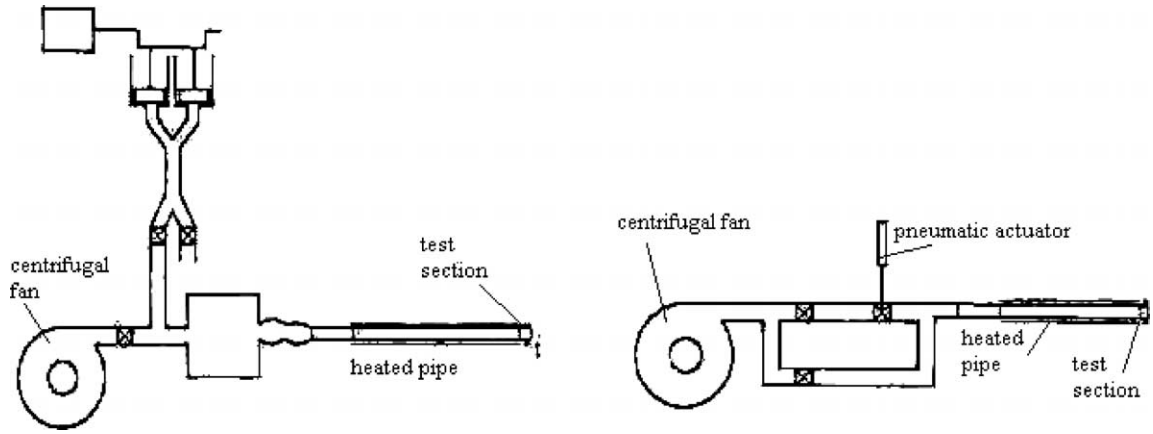

Fig. 1. Sketch of the test rig (left: sinusoidal perturbations, right: step changes) [8].

Table 1
Empirical and predicted Nusselt numbers

	$Re = 8000$	$Re = 30\,000$
Empirical Nusselt numbers:		
Nu, empirical	26.5	76.4
Predicted Nusselt numbers according to the turbulence model:		
Standard k–ε, standard wall funct.	28.6 (+8%)	75.0 (−2%)
Standard k–ε, non-equilibrium wall funct.	28.0 (+6%)	74.6 (−2%)
RNG k–ε, standard wall funct.	29.4 (+11%)	78.2 (+2%)
RNG k–ε, non-equilibrium wall funct.	28.8 (+9%)	77.4 (+1%)
Realizable k–ε, standard wall funct.	28.2 (+6%)	71.9 (−6%)
Realizable k–ε, non-equilibrium wall funct.	27.7 (+5%)	72.2 (−5%)
Spalart–Allmaras, vorticity based prod., st.wall f.	15.6 (−41%)	–
Spalart–Allmaras, strain based prod., st. wall f.	15.6 (−41%)	–
Standard k–ε, two-layer zonal near-wall model	29.1 (+10%)	79.4 (+4%)

The velocities and temperatures were measured using a hot-wire anemometer and a cold-wire resistance thermometer, respectively. The heat flux at the wall was measured with a sensor, based on the principle of finding the temperature difference over a known thermal resistance [8]. The measurements were performed at a test section near the pipe exit. The basic measured quantities displayed in [8] were the centreline flow velocity and the wall heat flux at the test section.

3.1. Steady state analysis

Before starting with the transient analysis, the steady-state heat transfer in turbulent pipe flow has been analysed. The steady-state analysis has been carried out for two extreme mean Reynolds numbers of the transient experiments, i.e., for $Re = 8000$ and $Re = 30\,000$. Steady-state results were not presented in the experiments [8]. However, it has been found that it would be useful to compare the predictions with the available correlations. For the convective heat transfer in steady-state, turbulent pipe flow under fully developed conditions, there are several correlations in the literature [17,18].

We consider here the following correlation, which, was also considered in [8], as a basis for some analysis of the experimental results.

$$Nu = 0.023\,Re^{0.8}Pr^{0.4} \tag{1}$$

Empirical Nusselt numbers obtained by Eq. (1), for the steady-state, fully developed turbulent pipe flow, for $Re = 8000$ and $Re = 30\,000$ are displayed in Table 1. However, since $Re \geqslant 10\,000$ was declared [18] as the validity range of Eq. (1), the value for $Re = 8000$ (Table 1) may be considered to be less reliable. The predicted Nusselt numbers using different turbulence models, for the steady-state, fully developed turbulent pipe flow, for $Re = 8000$ and $Re = 30\,000$ are presented in Table 1, as well, where percentage deviations from the empirical values are also indicated in brackets.

One observes that the one-equation Spalart–Allmaras model, used only for $Re = 8000$, adopting wall functions for the near-wall flow, predicts quite different values compared to the other models, which are obviously erroneous. This may be attributed to the fact that the model is originally a low-Reynolds-number one, and should be expected to deliver better results, using a sufficient grid resolution near the wall, instead of adopting the wall functions. It can be observed that for $Re = 8000$, all models over-predict

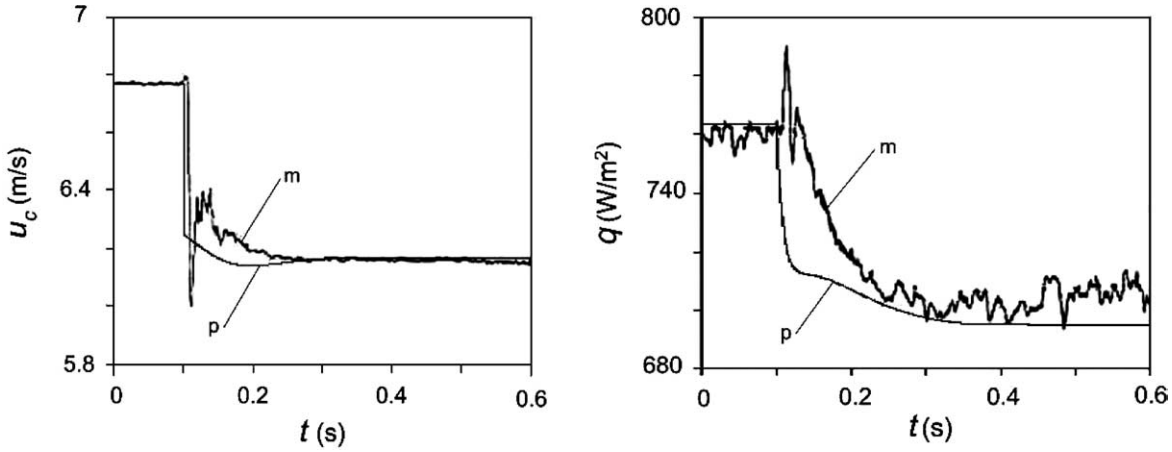

Fig. 2. Transient response to a step change in flow rate, left: centreline velocity, right: wall heat flux (p: predictions, m: measurements).

the empirical value, where the RNG k–ε model shows the highest deviation.

For $Re = 30\,000$, the RNG k–ε model and the standard k–ε model with two-layer-zonal near-wall model continue to over-predict the empirical value, whereas the others show an under-prediction. Furthermore, it can be observed that the use of "standard" or "non-equilibrium" wall functions does not have a substantial influence on the results. One can also observe that this influence is somewhat greater for $Re = 8000$ than for $Re = 30\,000$.

Direct experimental results were not available in [8], for the considered steady-state test cases. Thus, a very specific conclusion on the performance of the turbulence models cannot be drawn based on the present comparisons. Nevertheless, one may generally conclude that the considered two-equation models perform similarly well for $Re = 30\,000$, within a deviation range of approx. $\pm 5\%$ from the empirical value.

3.2. Transient analysis

In the transient analysis, the standard k–ε model with non-equilibrium wall functions has been used as the basic model. For some cases, other turbulence models including the one with two-layer-zonal near-wall treatment have also been employed, for investigating possible accuracy improvements.

3.2.1. Response to step changes

The transient responses of the centreline velocity and the wall heat flux at the test section, to a sudden reduction of the mass flow rate are shown in Fig. 2, where the predictions are compared with measurements [8].

For the velocity, the small "jump" after the sudden reduction has not been predicted. This, can, however, be due to the fact that the computations model an ideally "stepwise" sudden reduction of the flow rate, whereas the real transience might be deviating from that. Clearly, the velocity drop causes a drop in the wall heat flux as indicated by predictions and measurements. The predictions show a much steeper reduction in time, whereas the reduction indicated by measurements is slower, causing a discrepancy, especially for the first 0.1 seconds. This discrepancy is expected, at least partially, to be caused by the above-mentioned behaviour of the velocity. After about 0.1 seconds, the predicted value of the wall heat flux is rather close to the measurements, with a slight under-prediction.

3.2.2. Response to pulse-like changes

Transient responses of the centreline velocity and the wall heat flux, at the test section, to pulse-like changes in the flow rate, are shown in Fig. 3, for three Reynolds numbers of the undisturbed flow, namely for $Re = 8000$, $Re = 13\,500$ and $Re = 18\,000$.

For, $Re = 8000$, the predicted and measured heat flux curves do not agree very well. The predicted peak heat flux values agree rather well with the measurements, for $Re = 13\,500$ and $Re = 18\,000$. The experiments show a delay between the peak of the velocity and the peak of the heat flux, which is more significant at low Reynolds numbers, but tend to become smaller for higher Reynolds numbers. This delay has been strongly under-predicted by the simulations, which indicate a nearly simultaneous occurring of the velocity and heat flux peaks. Consequently, as far as this aspect is concerned, the agreement between the predictions and measurements, turns out to be better for $Re = 18\,000$.

3.2.3. Response to sinusoidal perturbations

Sinusoidal oscillations of the flow rate have also been investigated for the mean Reynolds number of $Re = 10\,500$ and the sinusoidal frequency of approximately 3 Hz. Different relative amplitudes of the oscillations, namely 10, 30, 50 and 80% have been considered.

Computation of oscillating cases with high amplitudes puts additional demands on the turbulence models and grids used. One must take care that the conditions for the application of wall-functions, or, for the two-layer-zonal

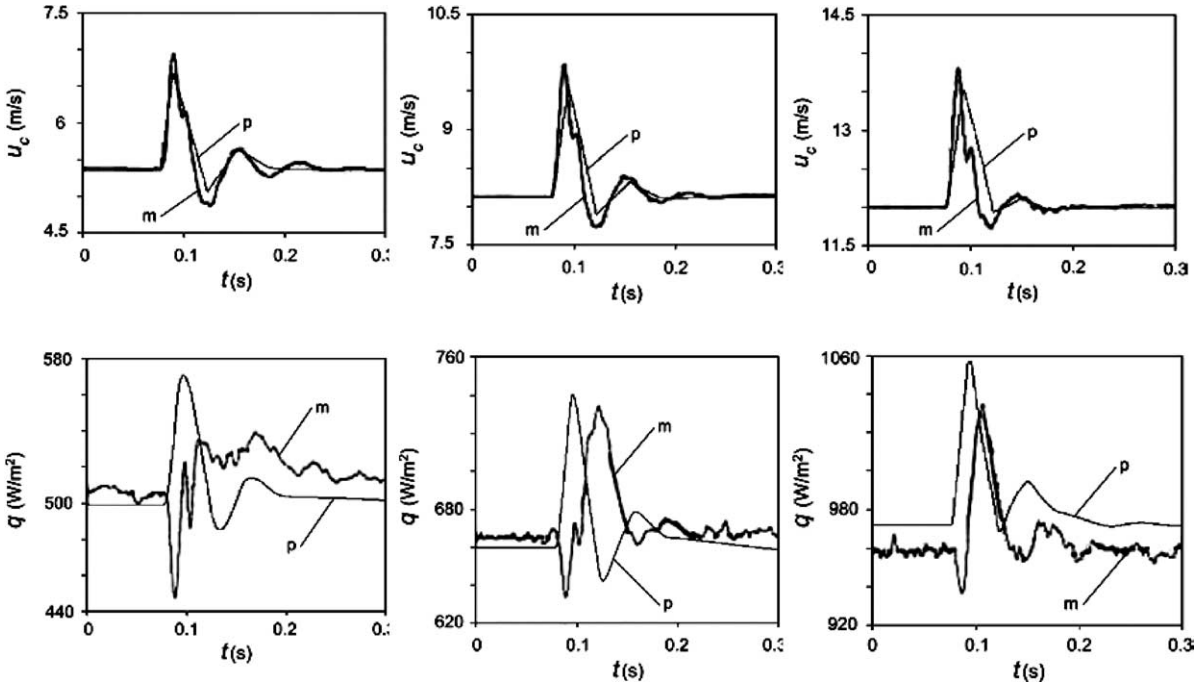

Fig. 3. Transient response to pulse-like changes. above: centreline velocity, below: wall heat flux, left: $Re = 8000$, middle: $Re = 13\,500$, right: $Re = 18\,000$ (p: predictions, m: measurements).

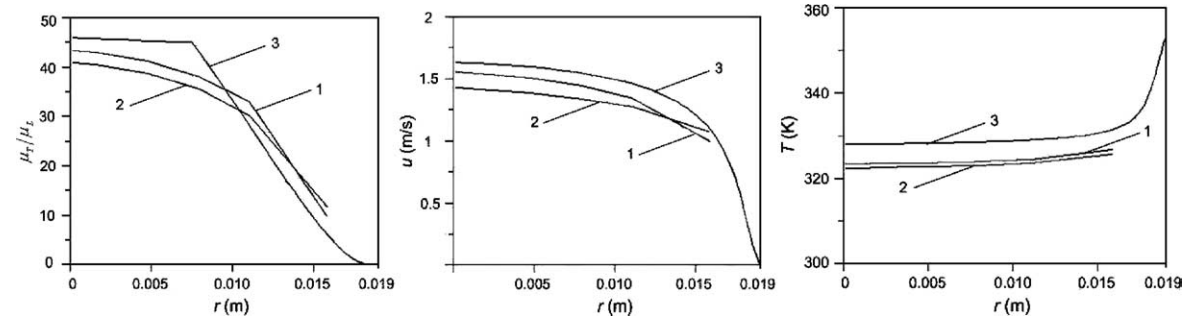

Fig. 4. Predicted radial profiles at measuring station for temporally minimum flow rate of 80% relative amplitude, left: viscosity ratio (μ_T/μ_L), middle: axial velocity, right: temperature, 1: Std. k–ε, std. wall-functions, 2: Std. k–ε, non-equilibrium wall-functions, 3: Std. k–ε, two-layer-zonal near-wall treatment.

method are not violated at the minimum and maximum values of the flow rate, respectively. In the present case, it was ensured that the condition of $y^+ > 15$ was fulfilled even for the minimum flow rates for the 80% relative amplitude, using the wall-functions approach. On the other hand, it was also ensured that the condition of $y^+ < 1.0$ was fulfilled even for the maximum flow rates for the 80% relative amplitude, when using the two-layer-zonal approach.

Radial profiles of the viscosity ratio (μ_T/μ_L), the axial velocity and the temperature at the measuring section, for the temporally minimum flow rate of 80% relative amplitude, as predicted by three turbulence models, are illustrated in Fig. 4.

For the predictions using the wall-functions method, the gap observed beyond the right-hand edge of the curves, in Fig. 4, indicate the near-wall region, which was not resolved by the grid, but modelled by the wall-functions approach. In Fig. 4, one can see that the models predict qualitatively quite similar curves, whereas remarkable local quantitative deviations within the range of approx. ±10% may also be observed. However, the wall heat flux values predicted by the three models have been rather close to each other, scattering within the range of approx. ±2%.

According to the predictions, the temporal oscillations have shown no substantial influence on the time-averaged heat transfer, for the considered cases. The time-averaged heat flux values for the oscillating cases were practically equal to that of the steady-state case values (the time-averaged wall heat flux exceeded the steady state value only by 1%, for the case with 80% relative amplitude). This finding is in agreement with the experimental observations [8].

The temporal variation of the centreline velocity and the wall heat flux for different relative amplitudes (10, 30, 50 and 80%) are illustrated in Fig. 5.

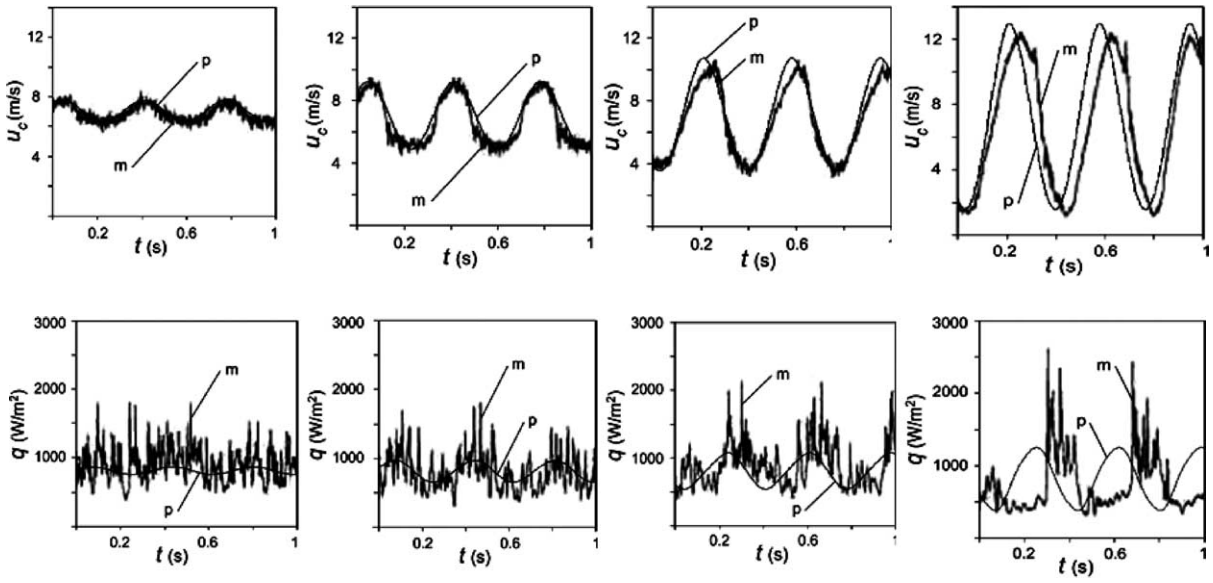

Fig. 5. Transient response to sinusoidal flow rate variations, above: centreline velocity, below: wall heat flux, relative amplitude: 10, 30, 50, 80%, from left to right (p: predictions, m: measurements).

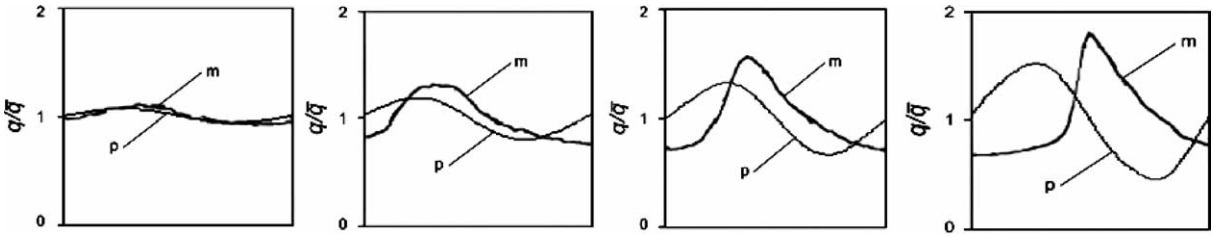

Fig. 6. Predicted wall heat flux compared with ensemble averaged measurements for one period, relative amplitude: 10, 30, 50, 80%, from left to right (p: predictions, m: measurements).

Table 2
Heat flux response delay time as fraction of period

	Delay time/period			
	10% amplitude	30% amplitude	50% amplitude	80% amplitude
Experiments	0.13	0.13	0.16	0.21
Predictions	0.04	0.04	0.05	0.06

The displayed measured values of the wall heat flux were obtained by a single measurement, and are highly oscillatory. A clearer comparison can be obtained based on the ensemble averaged measurements. Fig. 6 presents the predicted time variations of the heat flux, normalized by the time-averaged value, compared with those obtained by ensemble averages of the measurements (obtained by averaging for about 1000 ensembles), for the cases illustrated in Fig. 5, only for one period of time.

One can see in Fig. 6 that the peak values of the normalized heat flux are generally under-predicted up to 40% by the computations. Note that the experimental curve shapes are rather sinusoidal for low relative amplitudes (10%), but deviate from this form and become rather non-sinusoidal for higher relative amplitudes, especially for 50 and 80%. This may be attributed to increased low Reynolds number effects around temporally minimum flow rates, during the oscillations. For the predictions, this tendency is observed in a weaker manner for 80% relative amplitude.

One can see in Figs. 5 and 6 that there is a delay in the response of the wall heat flux to the velocity oscillations, especially for the high amplitudes, which is under-predicted by the computations. The predicted delay time of the wall heat flux to the velocity oscillations are compared with the measured values in Table 2, as fractions of a period. One can see that the modelling under-predicts the experimentally observed delay quite substantially.

This behaviour, i.e., the inability of the calculations to properly predict the delay in the response of the wall heat flux was also observed for pulse-like changes, especially for

those with smaller Reynolds numbers (Fig 3). Sinusoidal oscillations with different frequencies and amplitudes have also been analysed, where, quite similar tendencies have been observed, as far as the prediction of the delay time is concerned.

An explanation for the experimental wall heat flux lagging behind the velocity was given in [8], based on the consideration that the slow-moving fluid near the wall and the more energetic core region react differently to temporal changes of the flow rate.

However, a substantial effect due to such a mechanism has not been observed in the computations. As already mentioned above, different turbulence models with different near-wall treatments, including the two-layer-zonal ones, have also been applied, where no significant improvements of the prediction of the delay time have been observed. Furthermore, the influence of using different boundary conditions has also been investigated. The predictions shown, so far, were all obtained by prescribing time dependent mass flow rates at the pipe inlet, assuming a radially constant inlet velocity. Instead of this formulation, computations have also been carried out by prescribing time dependent, radially constant total pressures at the inlet, which allows more flexibility on the resulting velocity profile, and may be assumed to represent the physical conditions better. However, no improvements have been observed in the prediction of the above-mentioned delayed response of the heat flux to the flow rate changes.

4. Conclusions

Unsteady convective heat transfer in turbulent pipe flow has been investigated computationally by means of transient simulations. Different turbulence models have been used in the investigation. The transient analysis was preceded by a steady-state study, where no substantial differences in performances of the considered two-equation turbulence models were observed. In the transient analysis, the main emphasis has been placed upon high Reynolds number two-equation turbulence models, augmented by the wall-functions approach, where two-layer-zonal models, which do not utilize the wall-functions have also been considered for some cases. Step-like, pulse-like and sinusoidal perturbations of the flow rate at various Reynolds number have been investigated. Results have been compared with measurements. Predictions have indicated that the sinusoidal perturbations do not substantially influence the time-mean wall heat flux, for the considered cases. This has been in agreement with the experimental observations. For the pulse-like changes, the predictions showed some agreement in the shapes of the transient curves and in the peak values of the wall heat flux, whereas the agreement was better for higher Reynolds numbers. For the sinusoidal perturbations, the peak values of the wall heat flux were always under-predicted, the maximum deviation being about 40%. In puls-like and sinusoidal perturbations, experiments indicate a delay in the response of the wall heat flux to the changes of the flow rate, depending on parameters such as the mean Reynolds number, the relative amplitude, and frequency of the oscillations. This delay was strongly under-predicted by the modelling.

References

[1] J.E. Dec, J.O. Keller, Pulse combustor tail-pipe heat-transfer dependence on frequency, amplitude and mean flow rate, Combustion Flame 77 (1989) 359–374.
[2] R.C. Herndon, P.E. Hubble, J.L. Gainer, Two pulsators for increasing heat transfer, Industrial and Engineering Chemistry, Process Design Dev. 19 (1980) 405–410.
[3] P.J. Shayler, M.J.F. Colechin, A. Scarisbrick, Heat transfer measurements in the intake port of a spark ignition engine, SAE Trans. J. Materials Manuf. 5 (1996) 257–267.
[4] H. Dol, K. Hanjalic, S. Kenjeres, A comparative assessment of the second moment differential and algebraic models in turbulent natural convection, Internat. J. Heat Fluid Flow 18 (1997) 4–14.
[5] V.C. Patel, W. Rodi, G. Scheuerer, Turbulence models for near-wall and low Reynolds number flows—a review, AIAA J. 23 (1985) 1308–1328.
[6] J. Bredberg, L. Davidson, H. Iacovides, Comparison of near-wall behaviour and its effect on heat transfer for k–ω and k–ε turbulence models in rib-roughened channels, in: Y. Nagano, K. Hanjalic, T. Tsuji (Eds.), Proceedings of the Third International Symposium of Turbulent Heat and Mass Transfer, 2000, pp. 381–388.
[7] W. Vieser, T. Esch, F. Menter, Heat transfer predictions using advanced two equation turbulence models, CFX Techn. Mem. CFX-VAL10/0602, AEA Technology, Otterfing, 2002.
[8] A.R. Barker, J.E.F. Williams, Transient measurements of the heat transfer coefficient in unsteady turbulent pipe flow, Internat. J. Heat Mass Transfer 43 (2000) 3197–3207.
[9] Fluent 6, User' Guide, Fluent, Lebanon, NH, 2002.
[10] B.E. Launder, D.B. Spalding, The numerical computation of turbulent flows, Comput. Methods Appl. Mech. Engrg. 3 (1974) 269–289.
[11] V. Yakhot, S.A. Orszag, Renormalisation group analysis of turbulence: I. Basic theory, J. Sci. Comput. 1 (1986) 1–51.
[12] T.H. Shih, W.W. Liou, A. Shabbir, J. Zhu, A new k–ε eddy-viscosity model for high Reynolds number turbulent flows, Comput. Fluids 24 (1995) 227–238.
[13] P. Spalart, S. Almaras, A one-equation turbulence model for aerodynamic flows, AIAA Report, No. 92-2439, 1992.
[14] S.E. Kim, D. Choudhury, A near-wall treatment using wall functions sensitized to pressure gradient, in: Separated and Complex Flows, in: ASME FED, vol. 217, ASME, 1995.
[15] M. Wolfstein, The velocity and temperature distribution of one-dimensional flow with turbulence augmentation and pressure gradient, Internat. J. Heat Mass Transfer 12 (1969) 301–318.
[16] A.C. Benim, M. Arnal, A numerical analysis of the labyrinth seal flow, in: S. Wagner, J. Hirschel, J. Périaux, R. Piva (Eds.), Proceedings of the Second European Fluid Dynamics Conference (Computational Fluid Dynamics '94), Wiley, Chichester, 1994, pp. 839–846.
[17] W.M. Kays, Convective Heat and Mass Transfer, McGraw-Hill, New York, 1975.
[18] H.D. Baehr, K. Stephan, Wärme- und Stoffübertragung, Springer, Berlin, 1994.